Population synthesis at short wavelengths and spectrophotometric diagnostic tools for galaxy evolution

Alberto Buzzoni[1], Emanuele Bertone[2], Miguel Chávez[2,3], and Lino H. Rodríguez-Merino[2]

[1] INAF - Osservatorio Astronomico di Bologna, Via Ranzani 1 - 40127 Bologna, Italy - (e-mail: `alberto.buzzoni@oabo.inaf.it`)
[2] INAOE - Instituto Nacional de Astrofísica, Optica y Electrónica, Luis Enrique Erro 1 - 72840 Tonantzintla, Pue, Mexico - e-mail: (`ebertone@inaoep.mx`, `mchavez@inaoep.mx`, `lino@inaoep.mx`)
[3] IAM - Instituto de Astronomia y Meteorologia, Universidad de Guadalajara, Vallarta 2602 - 44130 Guadalajara, Mexico

Summary. Taking advantage of recent important advances in the calculation of high-resolution spectral grids of stellar atmospheres at short-wavelengths, and their implementation for population synthesis models, we briefly review here some special properties of ultraviolet emission in SSPs, and discuss their potential applications for identifying and tuning up effective diagnostic tools to probe distinctive evolutionary properties of early-type galaxies and other evolved stellar systems.

1 Introduction

With an amazingly successful series of dedicated space missions, the pioneering 70's marked the beginning of ultraviolet astronomy; satellites like ANS, OAO, and IUE opened the way, in fact, to the exploration of the nearby Universe at short spectral wavelength by-passing, for the first time, the blocking effect of Earth atmosphere. Since then, ultraviolet astronomy has received a renewed impulse in the current decade, partly due to on-going space projects like the GALEX mission or even the HST, but also under much different observational circumstances, as more powerful ground-based optical telescopes made the redshifted short-wavelength emission of distant galaxies to be eventually detectable at their visual-infrared eyes.

Curiously enough, we ended up by browsing ultraviolet features of galaxies at cosmic distances at much finer detail[4] compared to a still relatively scanty

---

[4] In addition, redshift acts on spectroscopic observations by improving wavelength resolution $\lambda/\Delta\lambda$ by a factor $(1 + z)$ in the galaxy restframe.

survey of the local stellar systems at wavelengths outside the optical range. For this reason, our understanding of the deep Universe cannot fully rely on a straightforward application of the local empirical templates, but rather needs an added value by theory to assess the evolution of high-redshift of stellar populations.

In this regard, population synthesis has attained nowadays an unprecedented accuracy in reproducing galaxy spectral features thanks to the match with increasingly refined libraries of stellar model atmospheres and improved algorithms to derive therefrom the high-resolution spectral information across the widest range of fundamental parameters (i.e. $\log T_{\mathrm{eff}}, \log g$, and [Fe/H]). As far as the short-wavelength range is concerned (i.e. for $\lambda \lesssim 3000$ Å) we can presently count on important theoretical datasets covering the full parameter space to reproduce stellar spectral energy distribution (SED) across the whole H-R diagram, at wavelength resolution typically better than $\lambda/\Delta\lambda \gtrsim 20\,000$ (see Bertone, 2005, for an exhaustive review on this subject). Among others, these include the work of Rodríguez-Merino et al. (2005) (Uvblue spectral library), Gustafsson et al. (2003) (Marcs model grid), Munari et al. (2005), Hauschildt et al. (1999) (the NextGen library), and Coelho et al. (2005).

As an effort to settle the interpretative framework that stems from the analysis of the short-wavelength SED of stellar systems, in this contribution we want to briefly review some special properties of ultraviolet emission in simple stellar populations (SSPs), and discuss their potential applications for identifying and tuning up effective diagnostic tools for population synthesis studies.

2 Short- vs. Long-term memory

It is commonly recognized that UV luminosity carries direct information on the age of young SSPs, being sensitive to the presence of hot and bright high-mass stars at the top main sequence (MS) turn-off (TO) point (e.g. O'Connell, 1999). While this certainly holds for a starburst case, where colors like $(U-V)$ are actually fair age tracers (see, e.g. Leitherer et al., 1999; Mas-Hesse & Kunth, 1991), things can be different, and subtly more entangled, in case star formation (SF) proceeds allover the galaxy life.

The key feature in this framework resides in a physically different "regime" of UV luminosity evolution compared to longer wavelengths. As far as the Johnson U band is concerned, for instance, models indicate that, for a solar metallicity and a Salpeter slope for the power-law IMF, SSP luminosity scales with time as

$$L_{\mathrm{SSP}}^{(U)} \quad \propto \quad t^{-1.1} \tag{1}$$

(see, e.g. Buzzoni, 2005). This holds over virtually the whole SSP history, from ages of a few Myr up to 10 Gyr and beyond (see Fig. 1).

If we assemble several equally mass-weighted SSPs (each producing stars up to a mass M_{up} with a fixed IMF) along a wider age range such as to
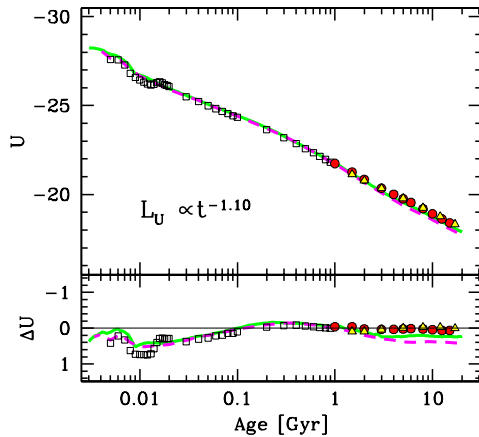
Fig. 1. Theoretical SSP luminosity evolution for solar metallicity and Salpeter IMF, according to different population synthesis codes, namely Buzzoni (1989, 2005) (dots), Worthey (1994) (triangles), Leitherer et al. (1999) (squares), Bressan et al. (1994) (dashed line), and Bruzual & Charlot (2003) (solid line). Absolute U magnitudes are scaled to a total SSP mass of 10^{11} M$_\odot$. For each model sequence, the residuals with respect to a perfect $L_U \propto t^{-1.10}$ trend are shown in the lower panel.

smoothly reproduce a constant SF rate over time t, then the total luminosity of the resulting composite stellar population (CSP) becomes

$$\mathcal{L}_{\mathrm{gal}}(t) \propto \int_{t_o}^{t} L_{\mathrm{SSP}}(\tau)d\tau = \int_{t_o}^{t} \tau^{-\alpha}d\tau = \frac{1}{1-\alpha} \quad \left[t^{1-\alpha} - t_o^{1-\alpha} \right]. \qquad (2)$$

In the equation, t_o is the lifetime of stars of highest mass, M_{up}, and can be operationally (and physically) conceived as the discrete integration time step $d\tau$ in each summation. If $\alpha < 1$, one sees that the r.h. solution of the integral is actually modulated by the *oldest* SSP components (that is those stars about t years old) as, in general, $t^{1-\alpha} \gg t_o^{1-\alpha}$. On the contrary, if the SSP luminosity fades more rapidly than $L_{\mathrm{SSP}} \propto t^{-1}$, that is for $\alpha > 1$, then the term $t_o^{1-\alpha}$ prevails and most of CSP luminosity comes from the *youngest* composing SSPs. In the latter case,

$$\mathcal{L}_{\mathrm{gal}} \propto \frac{t_o^{1-\alpha}}{\alpha - 1} = \mathrm{const.}(M_{\mathrm{up}}, \alpha) \qquad (3)$$

and the integrated CSP luminosity looses any dependence on age, only responding to the amount of short-lived high-mass stars, as modulated by the actual SF rate of the stellar aggregate (see Buzzoni, 2002, for a more detailed discussion). For the case of the U band $\alpha = 1.1$, and this is why ultraviolet luminosity is a so effective tracer of the *actual* SF activity carrying therefore "short-term" memory of the CSP history. More generally, α is expected to vary as a function of wavelength, as well, as the slope in the $\log L$ vs. $\log t$ relationship for a SSP depends on the relative contribution to total luminosity of stars in the different regions of the H-R diagram.

For the same reference SSP of Fig. 1, this is shown in Fig. 2 along the full spectral range. From the figure, one notes for example that eq. (3) holds
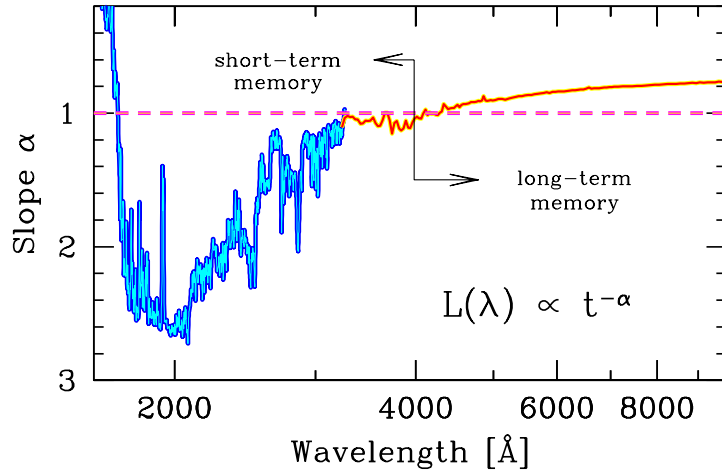
Fig. 2. Expected change with wavelength of the slope $\alpha = -\partial \log L(\lambda)/\partial \log t$ for a 15 Gyr SSP with solar metallicity, Salpeter IMF, and a red horizontal branch morphology, according to Buzzoni (1989). High-resolution UV synthesis made use of the Uvblue spectral library of Rodríguez-Merino et al. (2005). Note that α exceeds unity in the ultraviolet spectral region shortward of 4000 Å. As discussed in the text, this threshold value discriminates between two different regimes for SSP luminosity evolution.

along the entire mid-UV wavelength range, being $\alpha > 1$ for $\lambda \gtrsim 4000$ Å. On the contrary, the visual and infrared ranges characterize for a shallower SSP luminosity evolution ($\alpha < 1$). When applied to the case of a CSP, therefore, colors like $V - K$ are expected to carry "long-term" memory of CSP history through the cumulative effect of long-lived unevolved stars of low mass along the entire life of the stellar system.

The transition between short- and long-term memory regimes along SED of a CSP will also depend on the IMF details. Compared to the Salpeter case, for example, a stellar aggregate displaying a steeper (i.e. giant-dominated) IMF power slope would more likely wipe out any sign of its more remote past being populated at any time, on average, by shorter-lived higher-mass stars. In this case, α will exceed unity well longward of $\lambda \simeq 4000$ Å.

3 The Age-metallicity degeneracy

In spite of any more or less exotic recipe to combine stellar tracks and isochrones, from the physical point of view, the ultimate driving parameter that eventually constrains SED of a SSP is the mass of TO stars (M_{TO}). The latter will in fact set the cosmic clock (through MS stellar lifetimes) and reverberate on the overall morphology of the different evolutionary stages across

the synthetic H-R diagram of the SSP. As a major drawback of this situation, anytime we try to derive an absolute age estimate for the (either resolved or unresolved) SSP we also need to set *at the same time* its chemical composition. In other words, age and metallicity are intimately tied such as a wide range of SSPs can in principle give rise to fully equivalent spectrohotometric outputs.

More generally, synthesis models have extensively demonstrated that *"a factor of three change in age produces the same change in most colors and indices as a factor of two in Z"* (Worthey, 1992). So, old metal poor SSPs closely resemble in color and overall SED younger metal-rich ones. This effect, known as the "age-metallicity degeneracy" (Renzini & Buzzoni, 1986; Buzzoni, 1995), cannot easily be overcome as far as we restrain our analysis to the optical range of the SED of stellar systems, and we are forced therefore to browse the most extreme spectral windows, both at shorter and longer wavelength range, to break the "3-to-2" degeneracy and decouple, in principle, the t and Z pieces of information in SSPs. In this regard, ultraviolet is certainly a preferred window, in force of the more selective dependence of SSP luminosity on the upper MS stellar component.

Again, taking the SED of a 15 Gyr Salpeter SSP of solar metallicity as a reference, we have estimated in Fig. 3 the expected changes of total monochromatic luminosity along the entire SED vs. a change either in metallicity or age, assuming that

$$\begin{cases} L(15, Z) \propto L(15, Z_\odot) \left(\frac{Z}{Z_\odot}\right)^{-\beta(\lambda)} & \text{for fixed age, or} \\ L(t, Z_\odot) \propto L(15, Z_\odot) \left(\frac{t}{15\text{Gyr}}\right)^{-\alpha(\lambda)} & \text{for fixed metallicity.} \end{cases} \tag{4}$$

Worthey's steep slope $\Delta\beta/\Delta\alpha = \partial\log t/\partial\log Z \simeq \log 3/\log 2$ can easily be recognized for a long wavelength path spanning from the near infrared to the optical window, but a more complex behaviour begins to appear in the ultraviolet, especially in the Mid-UV range around the spectral region that roughly corresponds to the GALEX NUV pass-band, as displayed on the plot. The β vs. α curve then turns about 2000 Å changing direction with decreasing λ and eventually flattening shortward of 1500 Å.[5]

4 UV indices and SSP diagnostic

The recent theoretical grids of synthetic stellar atmospheres, covering the short-wavelength range at high spectral resolution, have made possible to

---

[5] Note that, contrary to the visual wavelenght range, age-metallicity degeneracy shortward of 2000 Å behaves in the opposite way, as the effect on FUV colors of a *younger* SSP can be recovered by *decreasing* metallicity.
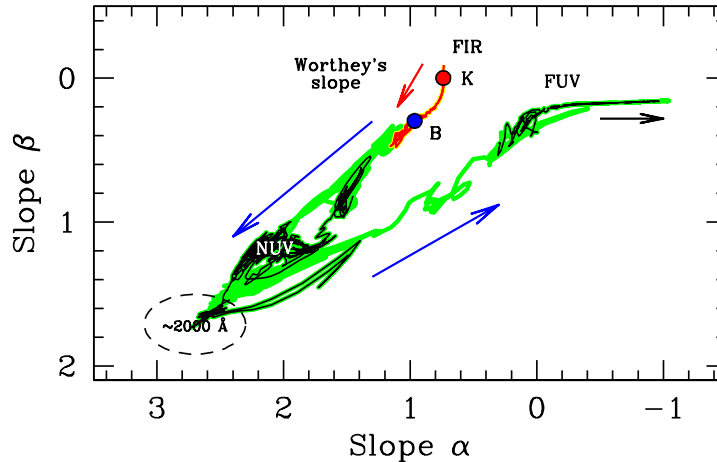
Fig. 3. Theoretical estimate of $\alpha = -\partial \log L(\lambda)/\partial \log t$ and $\beta = -\partial \log L(\lambda)/\partial \log Z$ slopes with varying wavelength from the infrared (Johnson K band at 2.2 μm) to the far ultraviolet ($\lambda \sim 1500$ Å), as indicated by the arrows, for the reference SSP of Fig. 2. Johnson B and K wave bands are labelled for reference on the plot, as well as the GALEX Far- (FUV) and Near-UV (NUV) bands. Note the turn-around feature about 2000 Å, and an opposite trend of the β vs. α relationship when moving toward the Far-UV spectral range. The Worthey (1992) "3-to-2" degeneracy vector is displayed on the plot (see text for a discussion).

directly trace the evolution of specific spectral features along the ultraviolet region of the SED of synthetic stellar atmospheres.

In particular, the mid-UV (i.e. 2200 $\lesssim \lambda \lesssim$ 3200 Å) wavelength range has been carefully screened by Chavez et al. (2007), based on the Rodríguez-Merino et al. (2005) UVBLUE spectral grid. The Chavez et al. analysis tackles, from the theoretical side, the original work of Fanelli et al. (1990), who carried out a comprehensive analysis of IUE stellar database through a set of narrow-band spectrophotometric indices able, in principle, to independently probe temperature, surface gravity, and chemical composition of stars. The big advantage of the theoretical approach, over the empirical one, however, is that one can more comfortably explore the change of spectral features with varying (in a controlled way) either one or more of the stellar fundamental parameters. In addition, also obvious limits of empirical samples can be overcome, like for instance the narrow range of [Fe/H] distribution, naturally peaked around the solar value when observing real stars in the solar neighbourhood.

The Chavez et al. (2007) theoretical framework has been further extended, by matching the UVBLUE spectral library with the Buzzoni (1989) population synthesis code to obtain synthetic UV indices for SSPs. Full details of this project are the subject of a forthcoming paper (Bertone et al., 2007), but we want to assess here just a few important issues related to a more refined use of
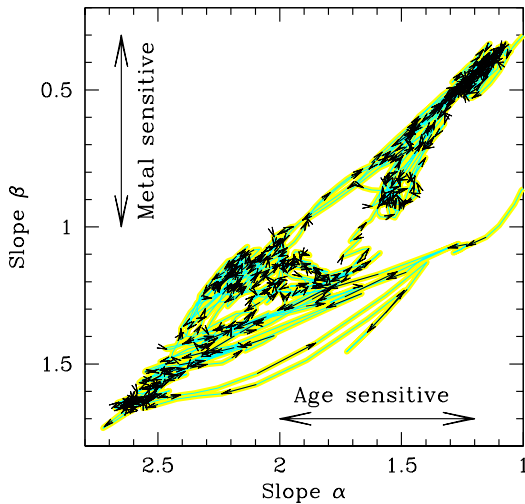
Fig. 4. A zoomed plot of the UV region from Fig. 3, sketching the trend of the $\Delta\beta/\Delta\alpha = \partial \log t/\partial \log Z$ degeneracy vector along wavelength, from 3000 Å (top right corner) to $\sim$ 1500 Å (mid-range curve to the right). According to the slope of the β vs. α relation, the different intervals of the UV SED can be selectively sensitive to either age ($\Delta\beta \to 0$) or metallicity changes ($\Delta\alpha \to 0$).

narrow-band indices *á la Fanelli* to probe evolutionary parameters of stellar populations. According to our previous discussion, as far as SSPs are concerned, the mid-UV spectral region appears to be the most promising one to break the "3-to-2" age-metallicity degeneracy. On a narrow-band wavelength scale like in Fig. 4, in fact, one can appreciate that the β vs. α correlation drastically deviates from the Worthey's slope, providing any sort of spectral "leverage" suitable to provide decoupled or even *orthogonal* pieces of information about age and metallicity. In this regard, by properly chosing both feature and pseudo-continuum bands, such as to have either a prevailing dependence on β or α, one could set up, in principle, new and optimzed narrow-band indices either metal- or age-sensitive, respectively.

On the same line, by means of Fig. 4 we could easily probe age- and metal-sensitivity of established narrow-band indices, like those in the Fanelli et al. (1990) system as well. Two interesting examples of nearly "horizontal" (i.e. most age-sensitive) and "vertical" (i.e. most metal-sensitive) indices are displayed in Fig. 5, for the case of the 2332 Å Fe II feature and for the 2538 Å metal blend.

Given its manifold piece of information, we are going to more systematically explore β vs. α diagnostic diagrams like those of Fig. 4 in order to identify and exploit potentially useful features to more cleanly probe distinctive properties of stellar population relying on the spectroscopic analysis of their integrated UV spectrum. To a more refined approach, however, such an excercise needs to more accurately size up the influence on Fig. 4 of theoretical uncertainties in high-resolution UV spectral synthesis, as well as the impact of other distinctive parameters of stellar aggregates, like the horizontal branch morphology, α-enhanced chemical partitions, and different slopes in the power-law IMF.
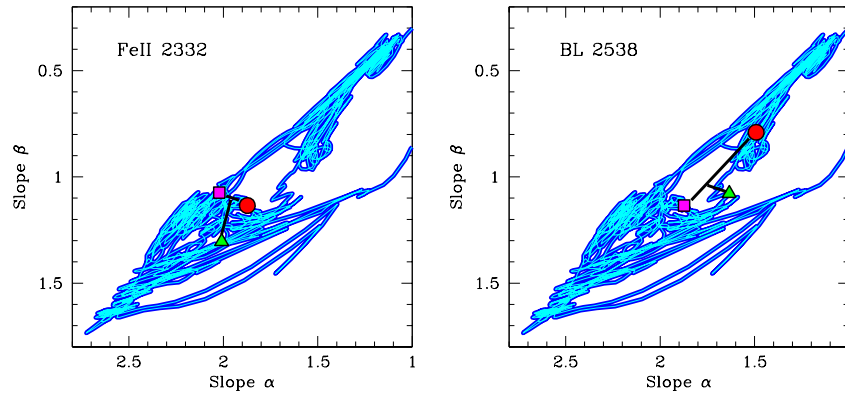
Fig. 5. Two illustrative cases of the Fanelli et al. (1990) narrow-band spectropho-
tometric indices located in the plot domain of Fig. 4. For the Fe II feature at 2332 Å
(left panel) and the metal blend about 2538 Å (right panel), the local degeneracy
vector $(\Delta\beta/\Delta\alpha)$ can be estimated by connecting the feature location (triangles on
the plots) with the corresponding pseudocontinuum, as interpolated from two "blue"
(squares) and "red" (dots) side bands. Note that, for its almost vertical slope, the
FeII index is better sensitive to metallicity, while thanks to a nearly horizontal trend,
the Bl 2538 index will better respond to any change in SSP age.

References

Bertone, E. 2005, Mem. SAIt Suppl. Ser., 8, 180
Bertone, E., Buzzoni, A., Chavez, M., Rodriguez-Merino, L.H. 2007, in preparation
Bressan, A., Chiosi, C., & Fagotto, F. 1994, ApJS, 94, 63
Bruzual, G., & Charlot, S. 2003, MNRAS, 344, 1000
Buzzoni, A. 1989, ApJS, 71, 817
Buzzoni, A. 1995, Fresh Views of Elliptical Galaxies, 86, 189
Buzzoni, A. 2002, AJ, 123, 1188
Buzzoni, A. 2005, MNRAS, 361, 725
Chavez, M., Bertone, E., Buzzoni, A., Franchini, M., Malagnini, M. L., Morossi, C., & Rodriguez-
    Merino, L. H. 2007, ApJ, 657, 1046
Coelho, P., Barbuy, B., Meléndez, J., Schiavon, R. P., & Castilho, B. V. 2005, A&A, 443, 735
Fanelli, M. N., O'Connell, R. W., Burstein, D., & Wu, C.-C. 1990, ApJ, 364, 272
Gustafsson, B., Edvardsson, B., Eriksson, K., Mizuno-Wiedner, M., Jørgensen, U. G., & Plez, B.
    2003, Stellar Atmosphere Modeling, 288, 331
Hauschildt, P. H., Allard, F., & Baron, E. 1999, ApJ, 512, 377
Leitherer, C., et al. 1999, ApJS, 123, 3
Mas-Hesse, J. M., & Kunth, D. 1991, A&AS, 88, 399
Munari, U., Sordo, R., Castelli, F., & Zwitter, T. 2005, A&A, 442, 1127
O'Connell, R. W. 1999, ARA&A, 37, 603
Renzini, A., & Buzzoni, A. 1986, Spectral evolution of galaxies, p. 195 - 235, 195
Rodríguez-Merino, L. H., Chavez, M., Bertone, E., & Buzzoni, A. 2005, ApJ, 626, 411
Worthey, G. 1992, Ph.D. Thesis, Univ. of California, Santa Cruz.
Worthey, G. 1994, ApJS, 95, 107